JTTEE5 19:1042–1053
DOI: 10.1007/s11666-010-9503-2
1059-9630/$19.00 © ASM International

Bactericidal Performance of Flame-Sprayed Nanostructured Titania-Copper Composite Coatings

N. George, M. Mahon, and A. McDonald

(Submitted December 13, 2009; in revised form March 18, 2010)

A large concern surrounding stainless steel surfaces is the ability of bacteria to grow and attach to them quite easily. One possible solution to destroy these pathogens is to coat surfaces with a biocidal agent. The photocatalytic effect of titanium dioxide (TiO_2) is known to have a bactericidal effect. Coatings of TiO_2 were prepared on 1010 low carbon steel substrates using an oxy-acetylene flame spray torch. TiO_2 coatings containing 5 wt.% copper (Cu) were fabricated to increase the bactericidal effect of the coating. After deposition, the coatings were polished to an average roughness of 1 μm. Solutions of *Pseudomonas aeruginosa* (PAK) bacteria were placed onto the coating surface for periods of up to 3 h, and the amount of surviving bacteria were counted. Some samples were irradiated with white light and other samples were held in a dark chamber. In coatings of copper-free flame-sprayed TiO_2, the high flame temperatures facilitated the conversion of the anatase phase to the rutile phase, which limited the photocatalytic destruction of the bacterial cells. However, TiO_2-copper composite coatings showed a large bactericidal effect, killing approximately 75% of PAK bacterial cells after 3 h. Under the same conditions, the TiO_2-copper composite coatings had the same bactericidal capabilities as pure copper surfaces, with the composite coatings showing improved bactericidal performance when exposed to light. It was proposed that increased concentrations of reactive oxide species produced due to TiO_2 photocatalysis improved the performance of the irradiated TiO_2-copper composite coatings.

Keywords anatase, copper, free radical, *Pseudomonas aeruginosa*, titania

1. Introduction

Bacterial growth on surfaces is a cause of concern in many food processing and hospital-based industries due to the possibility of increased risk of bacterial infection (Ref 1). *Pseudomonas aeruginosa* (*P. aeruginosa* or PAK) is an opportunistic pathogen that causes serious infections in intensive care and immunocompromised patients (e.g., cancer and AIDS) (Ref 2). These bacteria bind easily to stainless steel surfaces (Ref 3) to form highly organized communities known as biofilms (Ref 4). The thick biofilms provide improved protection and increase the survival rate of these micro-organisms. These biofilms mainly consist of a polysaccharide matrix, with β-1, 4 linked L-glucuronic and D-mannuronic acids, some embedded lipids, proteins, and nucleic acids (Ref 5). Micro-organisms that produce biofilms have increased resistance to several conventional methods of destruction, such as UV light exposure, metal toxicity, pH changes, dehydration, phagocytosis, and the use of antimicrobial agents (Ref 1).

Stainless steel is ubiquitously used throughout medical and food industries, and can serve as a reservoir to aid in the colonization of *P. aeruginosa* biofilms (Ref 3, 4). This has resulted in the need to develop novel coating or modified material surfaces with the innate capability of reducing bacterial growth. Previous studies have shown that titania (TiO_2) exhibits photocatalytic bactericidal properties (Ref 6-8). Photocatalysis is a process in which an illuminated substrate decomposes compounds by oxidation through acceleration of photoreactions. Thin film coatings of TiO_2, deposited through dip coating or chemical vapor deposition (CVD) were shown to kill *Escherichia coli* bacteria after 3 h (Ref 6, 7). Jeffery et al. (Ref 8) have shown that *P. aeruginosa*, a more complex and resilient micro-organism, was destroyed by a nanostructured TiO_2 coating surface fabricated by high-velocity oxy-fuel (HVOF) spraying—a thermal spraying process. In the study, approximately 25% of the bacteria exposed to the TiO_2 coating were destroyed after 2 h of white light ($\lambda = 400$-700 nm) exposure. The destruction of *P. aeruginosa* by the HVOF-sprayed nanostructured TiO_2 surfaces was attributed to the photocatalytic activity of the anatase phase of TiO_2.

The ability of TiO_2 to produce a photocatalytic effect sufficient to kill bacteria is dependent on the titania phases present. Amorphous TiO_2 presents no photoactivity. The rutile and anatase phases produce a photocatalytic effect, with the anatase phase being the predominant source of

N. George, M. Mahon, and **A. McDonald**, Department of Mechanical Engineering, University of Alberta, 4-9 Mechanical Engineering Building, Edmonton, AB T6G 2G8, Canada. Contact e-mail: andre.mcdonald@ualberta.ca.

photoactivity (Ref 9). Previous studies have shown that exposure of TiO_2 to high temperatures will result in phase transformation from the anatase to the rutile phase (Ref 9).

The destruction of micro-organisms by photocatalysis will involve many complex chemical reaction mechanisms. Upon illumination by ultra-violet (UV) or white light radiation, semiconductor materials such as TiO_2 create electron-hole pairs, which can generate reactive oxide species and free radicals such as hydroxyl radicals ($^{\bullet}OH$) from the oxidation of water present in solutions in contact with the surface (Ref 6). These radicals are oxidative, and are able to decompose many organic compounds found in bacteria and other micro-organisms (Ref 10). Metals such as silver have been combined with TiO_2 to enhance its antimicrobial properties (Ref 11). This enhancement of bactericidal behavior was attributed to the chemical toxicity of silver ions to bacteria and the photoactivity of TiO_2. The silver ions readily participated in auxiliary chemical reactions to destroy bacterial proteins and nucleic acids (Ref 12, 13). While silver possesses biocidal properties, it is expensive, even in small quantities. Therefore, other cheaper metals that are toxic to bacteria need to be considered as possible dopants in TiO_2.

Pure TiO_2 coatings have been fabricated by several methods, including CVD (Ref 11), PVD, HVOF thermal spraying (Ref 8, 14), and more recently, flame spray thermal spraying (Ref 15). Thin films of silver-TiO_2 composites have also been fabricated by the CVD process (Ref 11). The use of spray-dried agglomerated nanostructured TiO_2 particles in thermal spraying—a process in which a high temperature heat source is used to melt and accelerate powders to form coatings—has resulted in coatings with high adhesion strengths to steel surfaces and superior wear resistance (Ref 14) as compared to thin films deposited using CVD or PVD. The use of cost-effective thermal spraying processes to fabricate wear-resistant nanostructured TiO_2 coatings that possess photocatalytic capabilities to destroy bacteria such as *P. aeruginosa* can be a viable alternative to CVD or PVD-deposited thin films.

The present study is a continuation of the preliminary study conducted by Jeffery et al. (Ref 7). This research study investigates the possibility of using flame spraying to fabricate a metal-ceramic biocidal coating that combines the photocatalytic activity of TiO_2 and the bactericidal properties of copper metal.

2. Experimental Method

2.1 Thermal Spraying

Nanostructured titania (TiO_2) (TiCP2-P-01, Altair Nanotechnologies, Reno, NV) and conventional fused-and-crushed TiO_2 (Metco 102, Sulzer Metco Inc., Westbury, NY) were each deposited using an oxy-acetylene flame-spray torch (6PII ThermoSpray Gun, Sulzer Metco Inc., Westbury, NY). To fabricate all the coatings used in this study, the flame-spray torch was operated with acetylene at 22 SLPM (standard liters per minute) and oxygen at 35 SLPM. The powder carrier gas was argon at 9.5 SLPM (20 standard cubic feet per hour). The stand-off distance (distance between the torch and the substrate) was fixed at 100 mm. A robot (HP20, Motoman, Inc., West Carrollton, OH) operated at 400 mm/s was used to deposit the coatings in 24 passes.

The nanostructured and conventional TiO_2 powders were sieved with a Ro-Tap power siever (RX-29-CAN, W.S. Tyler, Mentor, OH) to obtain a powder size distribution of 18 to 38 μm (−38 + 18 μm). Copper (Cu) powder was added to the TiO_2 feed powder as a dopant for some coatings. The copper powder had a size distribution of 18 to 38 μm (−38 + 18 μm) and 5 wt.% was added to the TiO_2 powder to produce a mixture that was blended by hand for 15 min. Additional mixing occurred in the powder dispenser (5MPE, Sulzer Metco Inc., Westbury, NY) before deposition of the coating. All coatings were deposited onto grit-blasted 1010 low carbon steel (6511K51, McMaster-Carr, Los Angeles, CA) substrates measuring 4 by 51 by 83 mm. 1010 low carbon steel was chosen as the substrate to reduce or eliminate spallation of the TiO_2 coatings due to differences in the thermal expansion coefficients of the two materials.

To limit the amount of bacterial cells that remained on the surfaces during the tests, the coated samples were surface-finished before microbiological testing by polishing successively with 400, 800, and 1200 grit paper. It has been shown that reducing the surface roughness limited the ability of PAK to bind to surfaces (Ref 16). The surface roughness was measured using a surface profilometer (Esterline Federal Pocket Surf III EMD-1500-311, Mitutoyo, Aurora, IL).

2.2 Microbiological Testing

Once the coating samples were polished, they were washed using 500 μL of isopropanol and ethanol, respectively, to sterilize the surface and remove any contaminants. In order to contain the bacterial solutions on the coated substrates, Pyrex wells with 6 mm diameter and 8 mm height were mounted on the samples using silicone rubber (732 Multi-Purpose Sealant, Dow Corning, Midland, MI). A total of 15 wells were attached to each sample. These 15 wells allowed for results to be gathered in triplicate at time periods (t) of 0 to 4 h, in increments of 1 h. Time periods greater than 4 h were not considered due to possible desiccation of the bacterial solution. After 24 h, the samples were autoclaved (Amsco Century SG-120 Scientific Gravity Sterilizer, Steris Corporation, Mentor, OH) for 20 min at approximately 120 °C. The accuracy of the temperature measurement of the gravity sterilizer was ±1 °C. After sterilization, there were six samples. One sample each of conventional TiO_2-coated steel, nanostructured TiO_2-coated steel, and 304 stainless steel shim stock was exposed to cool white light (F40CW-RS-WM-Watt Miser, General Electric, New Haven, CT), and the rest was placed in a dark chamber.

Frozen stock of *P. aeruginosa* was scraped and placed in 4 mL of liquid broth (LB) to culture for 24 h at 37 °C in an incubator, to allow bacterial growth to reach a plateau.

When a sufficient amount of bacteria had grown, 50 μL of this solution was pipetted into 4 mL of LB and incubated for another four hours, so that the bacteria would be in the logarithmic stage of growth. In the following section, the bacterial concentrations will be reported per mL, but the final bacterial concentration will also be reported per 100 μL since that was the amount in each aliquot during the experiment. Using a photo-spectrometer, the concentration of the bacteria was measured and diluted with phosphate buffer saline (PBS) solution to an absorbency of 0.10, which created a stock solution of bacteria with a concentration on the order of approximately 10^7 cells/mL. For the experiments with copper-free flame-sprayed TiO_2, the bacteria underwent four consecutive dilutions with PBS solution, each reducing the concentration by a factor of 10, to obtain approximately 10^3 cells/mL. This final concentration of bacterial of 10^2 cells per 100 μL would facilitate cell counting. Experiments with flame-sprayed TiO_2-Cu composite coatings required larger concentrations of PAK. Instead of four, only two consecutive dilutions with PBS solution were completed, creating a final concentration of 10^5 cells/mL or 10^4 cells per 100 μL. As a result, whenever these aliquots for the flame-sprayed TiO_2-Cu composite coatings were removed from the wells, they had to be diluted twice more, each time by a factor of 10, to facilitate the cell counting process.

Once the final bacterial concentrations were reached, aliquots of 100 μL of bacterial solution were then pipetted into the wells on the surfaces. Immediately following this, the $t = 0$ h aliquots for all of the substrates were removed and plated onto brain-heart-infusion (BHI) 1.5% bacto-agar plates. Similarly, three separate aliquots of 100 μL were each plated directly onto BHI 1.5% bacto-agar plates, without touching the substrates, to establish a base count control of the bacteria that were placed onto the substrates.

Half of the substrates were placed in a dark chamber, and were not exposed to light. The other half were exposed to cool white fluorescent light ($\lambda = 400$-700 nm). At intervals of 1 h, up to a maximum time of 4 h, the appropriate aliquots were removed from the wells and plated onto BHI 1.5% bacto-agar plates. Following the removal of the aliquots, the BHI 1.5% bacto-agar plates were placed in an incubator at 37 °C overnight. Upon removing the agar plates, the quantity of Colony Forming Units (CFUs) for each agar plate were recorded in order to determine the bacterial population. It was assumed that each bacterium that was recovered from the substrates grew to form one colony or one CFU.

2.3 Coating Analysis

X-ray diffraction (RU-200B Line Focus X-Ray System, Rigaku Rotating Anode XRD System, Rigaku, Ontario, Canada) was used to identify the phases of TiO_2 that were present in the coatings. A continuous XRD mode, where the 2θ diffraction angle was changed from 10° to 110° at a rate of 2° per minute with a step size of 0.05° was used. Throughout the XRD tests, a copper anode was utilized at 40 kV and 110 mA.

A scanning electron microscope (SEM) analysis was conducted to ensure that the nanostructured TiO_2 coatings possessed nanostructured characteristics similar to those observed by Lima and Marple (Ref 14). A scriber was used to produce wear scars for scratch tests on the polished coatings. In addition, the SEM images, coupled with ImagePro (Media Cybernetics, Bethesda, MD) were used to analyze the thickness and the porosity of the coatings. For this analysis, 30 SEM images for the nanostructured TiO_2, and 20 SEM images for the conventional TiO_2 were examined through the Count and Measure functions in ImagePro.

3. Results

3.1 SEM Images of Copper-free TiO_2 Coatings

Coatings of nanostructured and conventional TiO_2 were deposited onto roughened 1010 low carbon steel. The bactericidal activity of the coatings was determined by measuring the amount of bacterial cells that were destroyed. Initial tests conducted with as-sprayed (unpolished, rough) coatings produced large variances in the amount of Colony Forming Units (CFU's) recovered from the coating surfaces. The average surface roughness (R_a) on the as-sprayed coatings was larger than 6 μm. The large variance of CFU recovered, coupled with the large coating surface roughness suggested that adhesion of the PAK bacterial cells was high. To avoid increased cell adhesion, all surfaces were ground and polished to an average roughness of $R_a \approx 1$ μm, which significantly reduced this variability.

Figure 1 shows SEM images of nanostructured and conventional TiO_2 coatings. The figure shows that the nanostructured TiO_2 coating is denser with fewer pores. Through ImagePro analysis of the SEM images, the porosity of the nanostructured TiO_2 coatings was found to be approximately $8 \pm 5\%$ ($n = 30$) and for the conventional TiO_2 coatings, approximately $20 \pm 8\%$ ($n = 20$). The standard deviations are reported with the averages of all parameters mentioned in this study.

Lima and Marple (Ref 14) have shown in a previous study that wear scars in nanostructured TiO_2 coatings are significantly smoother, with a smeared appearance, than those of conventional, fused-and-crushed TiO_2 coatings, which exhibited brittle fracture. The smeared appearance was attributed to the use of a nanostructured powder feedstock. Figure 2 shows wear scars on nanostructured (Fig. 2a) and conventional (Fig. 2b) TiO_2 coatings after scratch tests. The wear scars observed in the present study also exhibit similar characteristics. The wear scars of the coating produced from the nanostructured TiO_2 powder (Fig. 2a) are ductile when compared to that of the conventional TiO_2 coating (Fig. 2b). Since both coatings were sprayed and tested under similar conditions, it is assumed that this difference in wear scar morphology is linked to the nanostructured character of the feedstock powder.

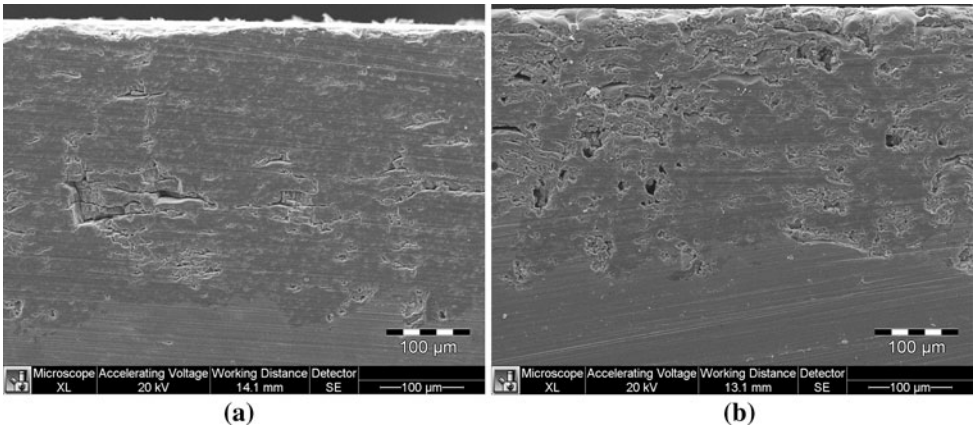

Fig. 1 Scanning electron microscope images of flame-sprayed (a) nanostructured TiO_2, one of 30 sample images, and (b) conventional TiO_2 coatings, one of 20 sample images

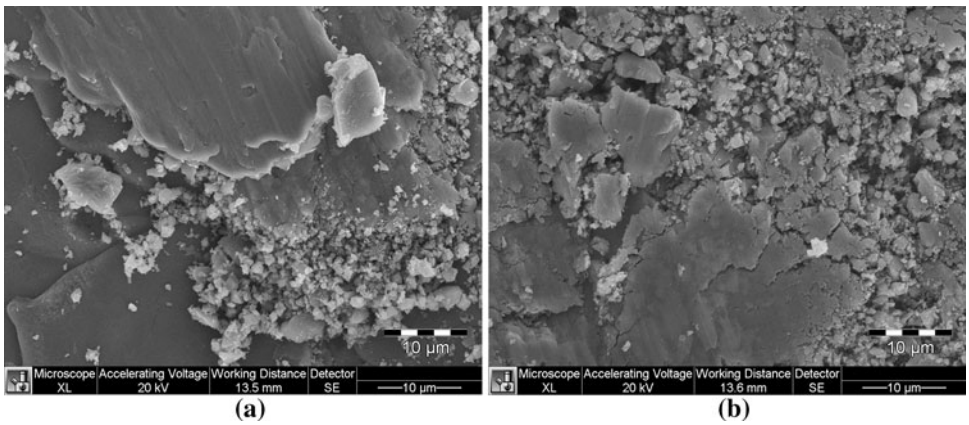

Fig. 2 Scanning electron microscope images of wear scars on flame-sprayed (a) nanostructured TiO_2 and (b) conventional TiO_2 coatings

3.2 Bactericidal Testing on Copper-free TiO_2 Coatings

The results of the bacterial killing assay performed on copper-free TiO_2 coatings and a stainless steel control are presented in Fig. 3. This figure shows the average number of CFUs recovered from the nanostructured and conventional TiO_2 and stainless steel surfaces after exposure to the surfaces over a 3-h period. Some samples were exposed to white light; others, were held in a dark chamber. It was assumed that each CFU was equivalent to one surviving bacterial cell. Error bars depicting the standard deviation are also shown. For each point shown in the curves of bacterial cells recovered in this study, $n = 3$. In the figure, a constant number of CFU's for a control sample of PAK cells that were not exposed to any of the surfaces is presented. The initial number of CFU's per 100 µL aliquot was approximately 185 (at $t = 0$ h). In the case of nanostructured TiO_2 over the 3-h period, the number of CFU decreased from 195 ± 8 to 95 ± 1 CFU, for the light-exposed samples, and from 195 ± 8 to 107 ± 56 CFU, for the samples held in the dark chamber (Fig. 3a). Similarly, for the conventional coating after 3 h, the number of CFU decreased from a 187 ± 14 to 119 ± 17 CFU and to 77 ± 2 CFU, for the light-exposed and the dark chamber samples, respectively (Fig. 3b). Figure 3(c) shows that on the stainless steel surfaces exposed to white light or held in the dark chamber, the number of cells recovered per hour was approximately equal. Overall, there was a slight decrease from 200 ± 26 to 161 ± 35 CFU and 148 ± 8 CFU, for the light-exposed and the dark chamber samples, respectively, over a 3-h period. On the stainless steel surface, the number of CFU's recovered at each hour over the testing period was close to the control samples that were not exposed to any surfaces (see Fig. 3c).

3.3 X-Ray Diffraction (XRD) Analysis of Copper-free TiO_2 Coatings

XRD patterns of the nanostructured and conventional TiO_2 powders and coatings are shown in Fig. 4. An XRD analysis was completed to identify the phases of TiO_2 that were present before and after flame spray deposition of the coatings. The XRD pattern for both the nanostructured and conventional TiO_2 stock powder showed that

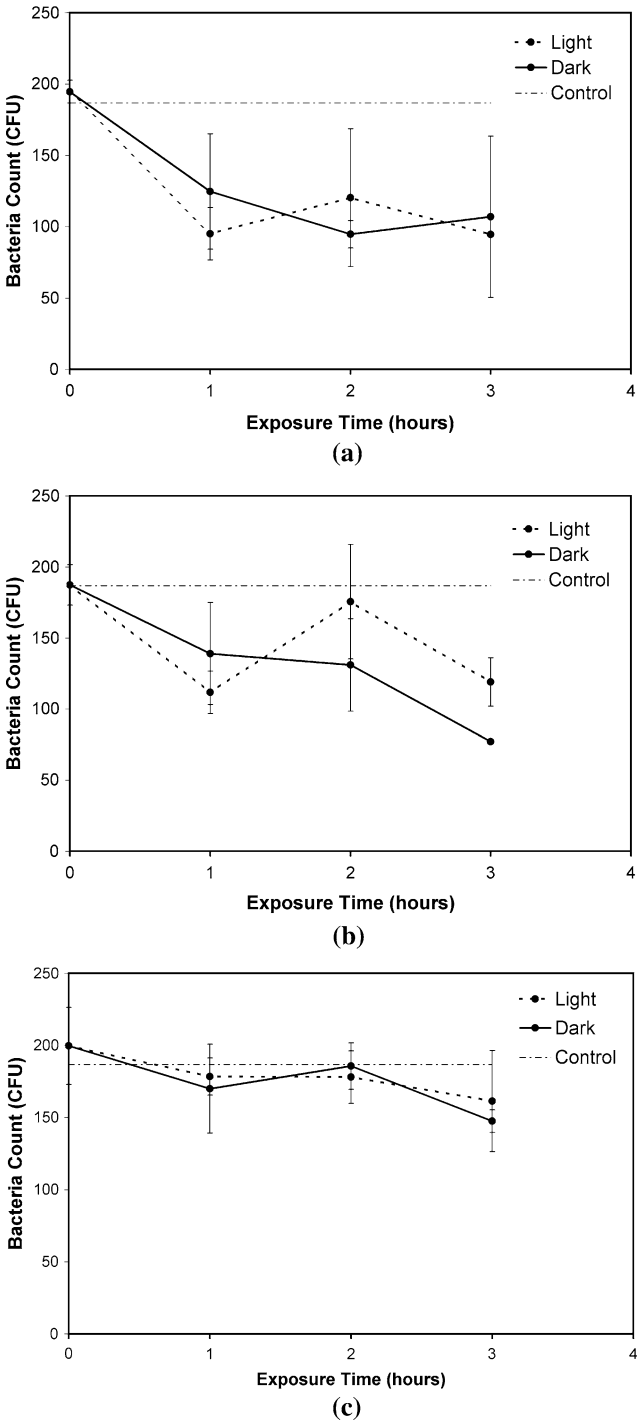

Fig. 3 Bacterial cells recovered from (a) flame-sprayed nanostructured TiO_2 coating (b) flame-sprayed conventional TiO_2 coating, and (c) uncoated 304 stainless steel

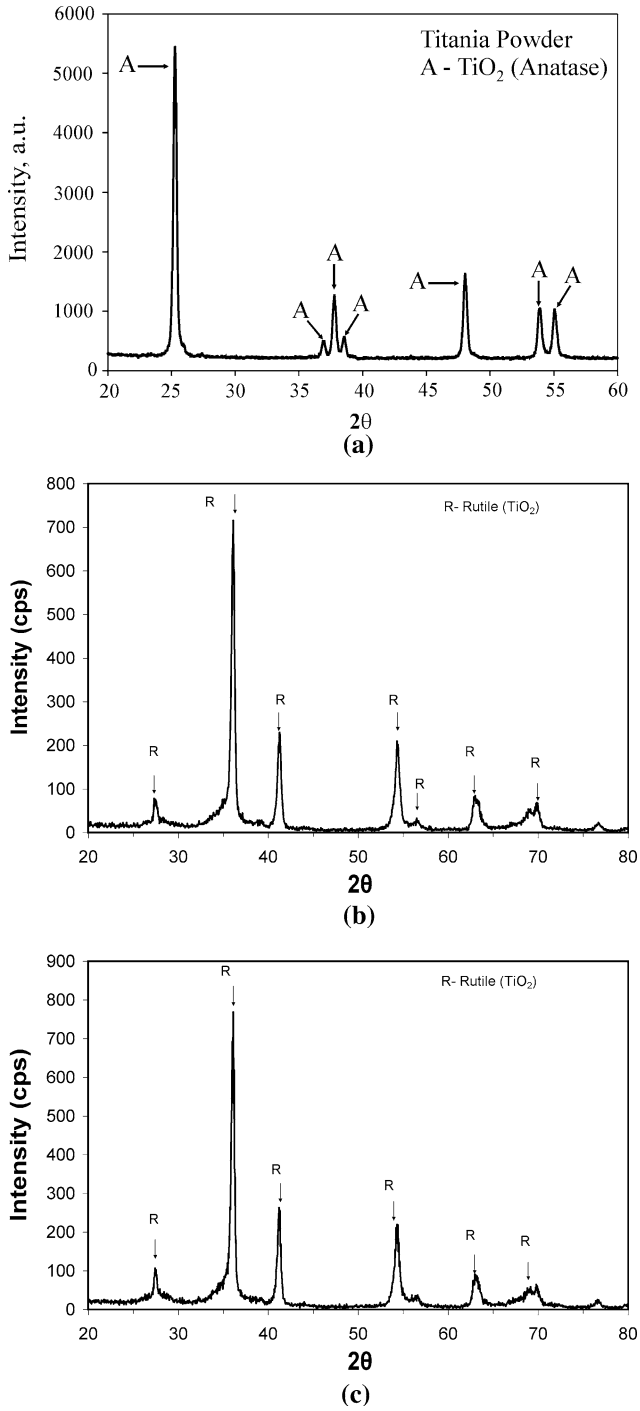

Fig. 4 Typical XRD patterns of (a) initial TiO_2 powder [8], (b) flame-sprayed nanostructured TiO_2 coating, and (c) flame-sprayed conventional TiO_2 coating

the powder consisted of 100% anatase phase (Fig. 4a) (Ref 8). In comparison, the XRD patterns for the flame-sprayed, copper-free TiO_2 coatings show no observable anatase phase. Rather, only the rutile phase is present (Fig. 4b, c). The figure also shows that no brookite or sub-oxide phases are present.

3.4 Bactericidal Testing on TiO_2-Copper Composite Coating Surfaces

An objective of this study was to investigate the possibility of fabricating high-performance flame-sprayed TiO_2-copper composite coatings. Aliquots of a 1000 CFU/mL bacterial solution were placed on composites of 5 wt.%

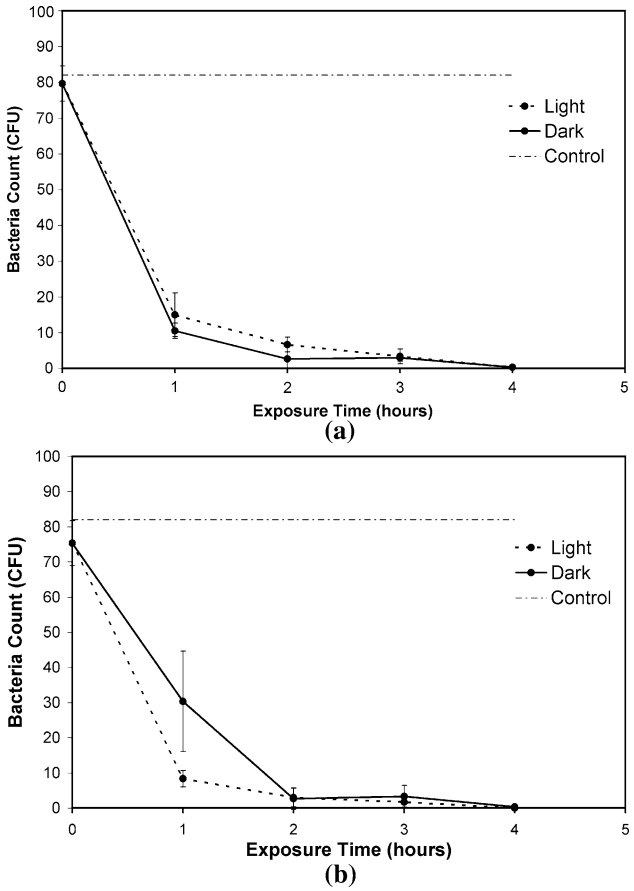

Fig. 5 Bacterial cells recovered from flame-sprayed (a) nanostructured TiO_2 coating and (b) conventional TiO_2 coating containing 5 wt.% Cu (Initial CFU: order of 100)

copper with nanostructured TiO_2 or conventional TiO_2. Figure 5 presents the results of the amount of bacterial cells recovered after one-hour intervals for 4 h. Based on the results shown, within 2 h, the number of CFU's of PAK bacteria recovered decreased from approximately 80 ± 5 to 7 ± 2 CFU on the nanostructured TiO_2 coating (Fig. 5a) and from 75 ± 6 to 3 ± 2 CFU for the conventional TiO_2 coating surfaces (Fig. 5b) that were exposed to white light. For the samples in the dark chamber, over the same time period, the number of CFU's decreased from 80 ± 5 to 3 ± 4 for the nanostructured TiO_2 coating, and from 75 ± 6 to 3 ± 3 CFU for the conventional TiO_2 coating. Although minute differences exist between the samples exposed to white light and those held in the dark chamber, similar results were observed. After 4 h, no cells were recovered from the coating surfaces.

The slopes of the curves shown in Fig. 5 are larger than those of the curves presented in Fig. 3, indicating that the rate of destruction of PAK was probably larger on TiO_2-Cu composite coatings. The slope of the curves in Fig. 5 also changed significantly throughout the experiment. It was unclear if the sharp changes in the slopes of these curves were significantly influenced by the low concentration of PAK bacterial solutions that were placed on the coatings. Previous studies (Ref 11, 17) have shown that larger concentrations of bacteria in solution will increase the kill time required. In order to verify whether the concentration of PAK influenced the bactericidal performance of the TiO_2 coatings, experiments with larger quantities of bacterial cells were conducted. It was also necessary to determine if these surfaces were able to eradicate higher concentrations of bacteria.

In a preliminary test, the number of CFUs per mL was increased from 10^3 to 10^5, which represents a change from 10^2 to 10^4 CFU per 100 μL aliquot. As shown in Fig. 6, the bactericidal performance of the flame-sprayed TiO_2-Cu composite coatings was compared with controls of stainless steel and pure copper plates. The TiO_2-Cu composite coatings and pure copper surface showed a significant decrease in the number of CFU's recovered. On the other hand, the stainless steel samples maintained a relatively constant number of bacteria over the time period of the experiment. Further, and similar to Fig. 3(c), the number of CFU's recovered at each hour over the testing period was close to the control samples that were not exposed to any surfaces (Fig. 6c). Unlike the other three graphs presented in Fig. 6, the results for nanostructured TiO_2-Cu composite coating (Fig. 6a) had a different control value since it was done in a separate experiment. The figure shows that results were obtained for 4 h of exposure. The fourth hour demonstrates that the trend for the nanostructured TiO_2-Cu composite coating is reliable. The nanostructured TiO_2-Cu composite coating showed a decrease over 4 h from approximately 8,350 to 650 CFU's for the samples exposed to white light, and from 7,100 to 1,500 CFU's for those samples held in the dark chamber (Fig. 6a). The conventional TiO_2-Cu composite coating showed a decrease from approximately 19,600 to 5,167 CFU's for the samples exposed to white light, and from 18,200 to 9,033 CFU's for those samples held in the dark chamber after 3 h (Fig. 6b). The number of CFU's recovered from the stainless steel control surfaces showed little overall change for both cases of light exposure and dark chamber tests (Fig. 6c), with the light-exposed samples showing a decrease in bacterial cells from 17,700 to 17,500 CFU's and for the dark chamber samples, a decrease from 16,133 to 11,400 CFU's over the 3-h period. The pure copper surface showed a decrease similar to that of the conventional TiO_2 coating after the 3-h period with a change from 18,967 to 6,933 CFU's on the white light-exposed samples, and from 18,967 to 4,767 CFU's on the samples held in the dark chamber (see Fig. 6d).

3.5 X-Ray Diffraction (XRD) of TiO_2-Copper Composite Coatings

Figure 7 shows the XRD patterns for the nanostructured and conventional TiO_2-Cu composite coatings. These XRD patterns show that small differences exist between the two types of composite coatings. However, in contrast to the copper-free TiO_2 coatings, noticeable amounts of anatase and copper (II) oxide (CuO) were found. The approximate volume percentage of anatase

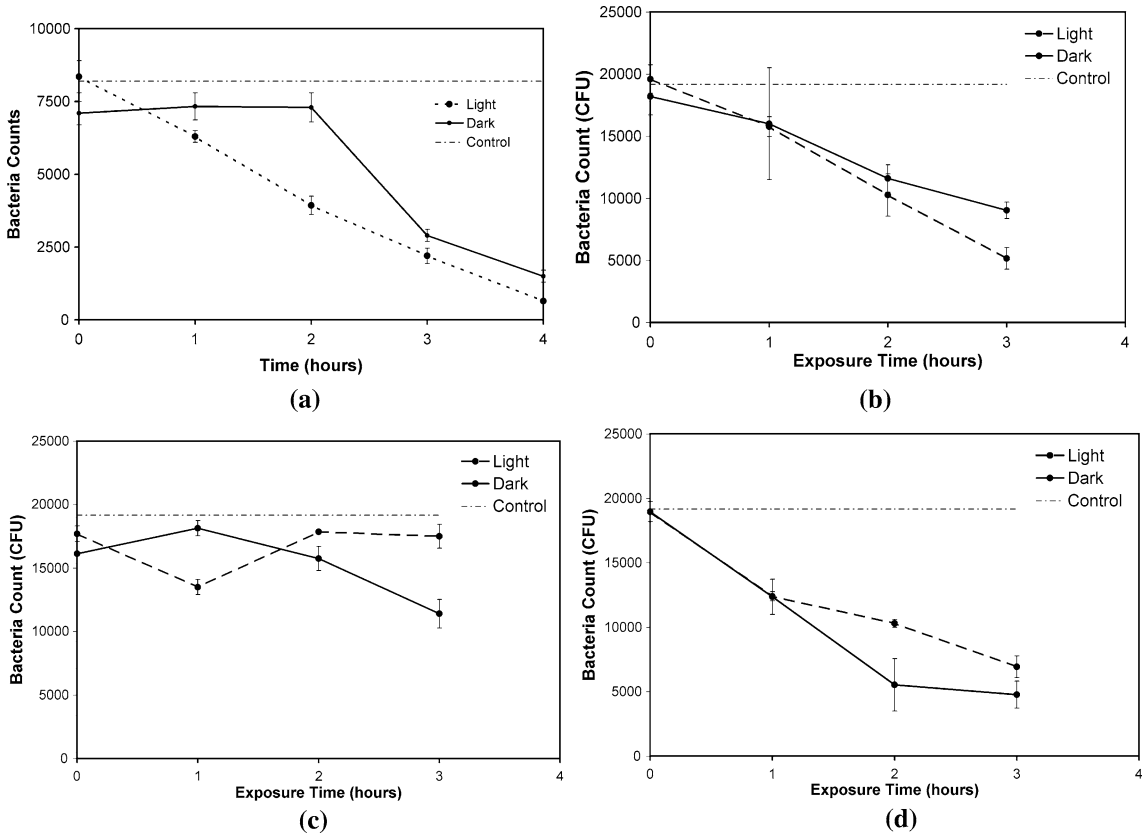

Fig. 6 Bacterial cells recovered from (a) flame-sprayed nanostructured TiO_2 coating containing 5 wt.% Cu, (b) flame-sprayed conventional TiO_2 coating containing 5 wt.% Cu, and controls of (c) 304 stainless steel, and (d) pure copper. (Initial CFU: order of 10,000)

present was determined by using the equation developed by Berger-Keller et al. (Ref 18):

$$C_A = \frac{8I_A}{(13I_R + 8I_A)} \times 100,$$

where I_A and I_R are the XRD intensities of the anatase (101) and rutile (110) peaks, respectively. The volume percentage of anatase in the composite coatings was approximately 9 vol.% anatase for both the nanostructured TiO_2 coating (Fig. 7a) and the conventional TiO_2 coating (Fig. 7b). The percentage of anatase calculated by the equation above is approximate since a small amount of copper (5 wt.%) was present in the microstructure. The equation applies when only the peaks of the anatase and rutile phases are present on the XRD profile.

4. Discussion

The results from microbiological testing of copper-free flame-sprayed TiO_2 coatings and stainless steel controls were analyzed to understand better the biocidal performance of the surfaces. The number of CFU recovered from both the nanostructured (Fig. 3a) and the conventional TiO_2 coatings (Fig. 3b) showed a significant decrease over the 3-h period. The decrease in the CFU count on the TiO_2 samples may be due to photocatalysis. However, comparison of the results obtained from the samples held in the light and those held in the dark chamber reveals that the number of CFU's recovered after each hour of exposure are close, and are statistically the same due to the size of the error bars. On the nanostructured TiO_2 coatings (Fig. 3a), the maximum difference in the CFU recovered between the samples exposed to white light and those held in the dark chamber was 30 CFU's, and this occurred after 2 h of testing. Likewise, for the conventional TiO_2 coatings (Fig. 3b), the maximum difference occurred after 2 h of testing, and was approximately 45 CFU's. The small differences between the light-exposed samples and those held in the dark chamber, coupled with the possibility of cell adhesion to the surfaces (Ref 8), is an indication that limited photocatalysis occurred. Instead, the observed decrease may be due to destruction of the bacterial cells as a result of starvation or dehydration or adhesion to the surfaces.

The decrease in the number of CFU's recovered from the stainless steel samples (Fig. 3c) was small for both the white light-exposed and dark chamber samples. Also, the difference between the two sets of results for the stainless steel was negligible. Any decrease was probably due to the active binding of PAK bacterial cells to the steel surfaces. It has been shown that PAK has high affinity for stainless steel (Ref 3), resulting in recovery of less bacteria from

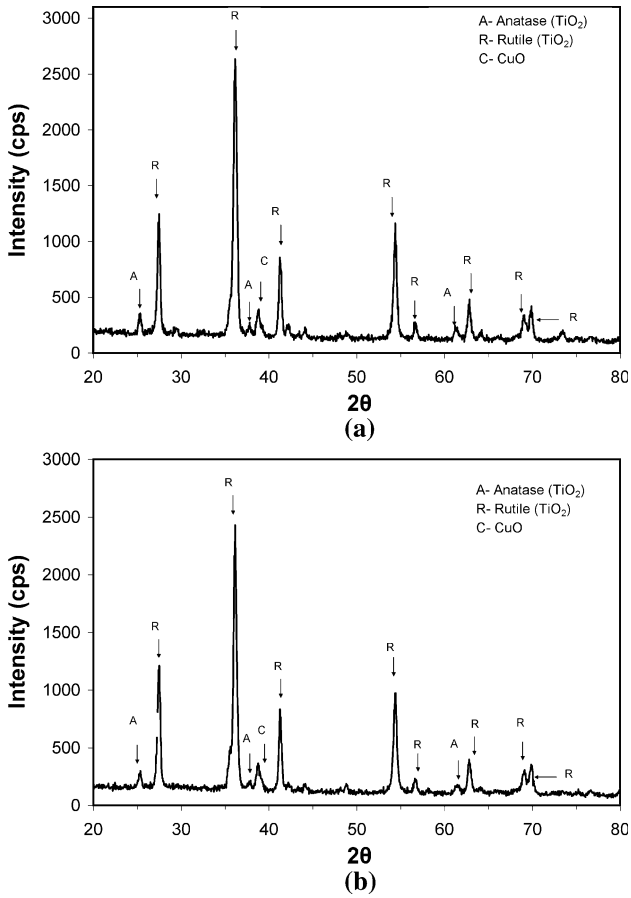

Fig. 7 Typical XRD patterns of polished flame-sprayed (a) nanostructured TiO_2 and (b) conventional TiO_2 coatings containing 5 wt.% Cu

those surfaces. Further analysis of Fig. 3 shows that approximately 50% of the original number of CFU's were unrecovered from the TiO_2 surfaces after 3 h, while 25% of the original number of CFU's were unrecovered from the stainless steel surfaces. A larger number of unrecovered bacterial cells from the TiO_2 surface was also observed by Jeffery et al. (Ref 8). The large number of PAK bacterial cells that were unrecovered from the TiO_2 surfaces was probably due to loss in the open pores of the coating (8% porosity) and/or chemical and mechanical adhesion to the surface.

Photocatalytic activity of TiO_2 occurs when white light is absorbed by the semi-conductor. The band gap values of the rutile and anatase phases are 3.0 and 3.2 eV, respectively (Ref 9, 19). Assuming that Planck's constant is 6.63×10^{-34} m^2 kg/s, the speed of light in a vacuum is 3.0×10^8 m/s, and 1 eV = 1.60×10^{-19} J, the absorbance range of TiO_2 is about 388 to 415 nm. Since the wavelength range of normal white light is 380-750 nm, it is expected that the TiO_2 coatings will exhibit some photocatalytic bactericidal activity. However, previous studies have shown that the anatase phase of TiO_2 is the dominant phase that produces the photocatalytic properties of this material (Ref 9, 20).

Jeffery et al. (Ref 8) and Amézaga-Madrid et al. (Ref 21) have suggested that the presence of the anatase phase in TiO_2 coatings and thin films contributed significantly to the observed destruction of PAK bacteria on these surfaces. In the study conducted by Jeffery et al. (Ref 8), the HVOF thermal spray process was used to fabricate the coatings. Flame temperatures in HVOF spraying are usually on the order of 2,000 K (Ref 22), higher particle velocities are produced, and the residence time of the particles in the hot flame are lower compared to other thermal spray processes. Phase transformation from the meta-stable anatase phase in the original stock power (see Fig. 4a) to the stable rutile phase will occur when the particle temperature exceeds approximately 1,100 K (Ref 23). The low thermal conductivity of TiO_2 (order of 10 W/m K compared to 400 W/m K for copper metal), coupled with the lower temperature and particle residence time in the HVOF spray flame, reduced the complete transformation of the anatase to rutile phase.

In the present study, oxy-acetylene flame spraying was used to fabricate the coatings. Flame temperatures in oxy-acetylene flame spraying have been shown to be on the order of 500 to 4,000 K (Ref 24). The particle velocities are typically lower in the flame spraying process than those in the HVOF spraying process, which results in longer particle residence times in the hot flame. Due to the high temperatures and longer particle residence times, conversion of the meta-stable anatase phase to the stable rutile phase was more pronounced. Figure 4 shows that the crystalline phase in the original TiO_2 stock powders was anatase. After deposition by flame spraying, complete transformation had occurred to the rutile phase (see Fig. 4b, c). The lack of anatase phase in the flame-sprayed coating resulted in limited killing of PAK, as observed in Fig. 3. These results suggest strongly that flame-sprayed TiO_2 alone will not achieve the bactericidal effect observed with HVOF TiO_2 coatings developed by others (Ref 8).

It has been well established that copper metal possesses anti-bacterial properties (Ref 25). Doping flame-sprayed nanostructured TiO_2 with a small amount of copper should increase the bactericidal properties of the coatings, while retaining the enhanced mechanical properties observed by others for nanostructured TiO_2 (Ref 14). Consequently, 5 wt.% copper was blended with both conventional and nanostructured TiO_2 powder. The addition of copper to the flame-sprayed TiO_2 coatings produced a dramatic increase in the killing rate of PAK (see Fig. 5 and 6). The results presented in Fig. 6 show that even with increased initial bacterial cell counts, on the order of 10,000 CFU, the amount of bacteria recovered from the TiO_2-Cu composite coating samples was substantially reduced after extended periods of exposure to the surfaces. This suggested that significant destruction of bacteria was occurring, rather than significant adhesion as observed in Fig. 3 for the copper-free TiO_2 coatings.

The results from the microbiological tests conducted with the larger (order of 10,000 CFU's) bacterial cell concentrations on TiO_2-Cu composite coatings further support the claim of photocatalytic bactericidal activity on

these surfaces. The amount of bacterial cells recovered from the composite coatings held in the dark chamber was, for the most part, higher than on those samples exposed to white light in the first hour of the test (Fig. 6a, b). For the TiO_2-Cu composite coatings after 3 h of testing, 700 additional CFU's of bacteria are recovered from the nanostructured TiO_2-Cu composite coatings held in the dark chamber (Fig. 6a) and 3,866 additional CFU's are recovered from the conventional TiO_2-Cu composite coatings (Fig. 6b). The additional bacterial cells destroyed by the TiO_2 coatings exposed to white light was probably due to the photocatalytic activity of the TiO_2 due to the presence of 9 vol.% anatase phase in the coating microstructure (see Fig. 7). Figure 6(d), which shows the number of bacterial cells recovered from the pure, bulk copper samples, indicates that 2,166 additional CFU's of bacteria were recovered from the samples exposed to white light 3 h of testing. This suggests that no photocatalysis occurred on the pure, bulk copper surfaces since the number of cells recovered from the surfaces held in the light were either equal to or greater than the number recovered from the copper samples held in the dark chamber. This difference between the pure, bulk copper samples and the TiO_2-Cu composite coating samples is a strong indication that photocatalysis by the TiO_2-Cu composite coating occurred in this study.

The XRD patterns presented for the copper-free TiO_2 coatings (Fig. 4) show 100 vol.% rutile and 0 vol.% anatase phases, while those of the TiO_2-Cu composite coatings (Fig. 7) show approximately 9 vol.% anatase phase. The peaks in Fig. 7, indicating the presence of CuO from oxidation of Cu, were expected due to the addition of the metal to the TiO_2 powder. The presence of the anatase phase in the composite coating was probably due to less energy available for anatase-rutile phase transformation since some of the energy was used to heat and convert Cu to CuO. Given that only 9 vol.% anatase phase was present in the final coating microstructure suggests that a limited amount of the total flame energy was transferred to the copper particles. Another plausible explanation may be that a small amount of Cu vaporized, cooling the flame. This reduced the energy of the flame needed to promote phase transformation from anatase to rutile in TiO_2. Additional studies need to be conducted in order to determine the exact reason for the anatase that remains in the flame-sprayed metal-TiO_2 composite coatings.

The controls used in this study were stainless steel and pure, bulk copper plates. Stainless steel was chosen since it is the material of choice in most food processing and medical industries. Copper plates were chosen to observe their ability to destroy PAK under the same conditions that were used with the flame-sprayed TiO_2 coatings. The stainless steel surfaces typically showed very small decreases in the number of CFU's of bacteria recovered over the period of the tests (Fig. 3 and 6), suggesting that limited bacterial cells were destroyed by the stainless steel controls. On the pure bulk copper control surfaces, there was a substantial decrease over the 3-h interval. If the standard deviation is considered, the results obtained on the samples exposed to white light and those held in the dark chamber were approximately equivalent (see Fig. 6d).

The increased bactericidal performance of flame-sprayed TiO_2-Cu composite coatings, especially those samples exposed to white light, was due to reactive species that attacked the PAK cells, resulting in their destruction. Copper ions and TiO_2 will probably participate in several chemical reaction mechanisms to produce the reactive species needed for cell destruction. Liochev and Fridovich (Ref 26) have shown copper-catalyzed Haber-Weiss reactions for the production of reactive oxygen species. In this present study, the reaction mechanism involving copper oxide (CuO) to form reactive species for PAK destruction may proceed as follows:

$$CuO(s) \leftrightarrow Cu^{2+}(aq) + O^{2-}(aq) \qquad K_{eq} = 8.4 \times 10^{-10} \tag{Eq 1}$$

$$O_2(g) + e^- \leftrightarrow O_2^-(aq) \tag{Eq 2}$$

The equilibrium constant, or solubility product, for reaction (1) is not typically found in most general references on general chemistry. However, McDowell and Johnston (Ref 27) have shown that the solubility of CuO in pure water at 25 °C is on the order of 2.9×10^{-5} mol/L. For reaction (1), K_{eq} is the product of the concentrations of the Cu^{2+} and O^{2-} ions, giving $K_{eq} = 8.4 \times 10^{-10}$.

Water may dissociate to facilitate the production of dihydrogen peroxide (H_2O_2):

$$H_2O(l) \leftrightarrow H^+(aq) + OH^-(aq) \qquad K_{eq} = 1.0 \times 10^{-14} \tag{Eq 3}$$

$$O_2(g) + 2H^+(aq) + 2e^- \leftrightarrow H_2O_2(aq) \qquad K_{eq} = 3.0 \times 10^{23} \tag{Eq 4}$$

The cupric ions (Cu^{2+}) produced in reaction (1) will react with the superoxide ions (O_2^-) produced in reaction (2) to facilitate production of reactive species:

$$Cu^{2+}(aq) + O_2^-(aq) \leftrightarrow Cu^+(aq) + O_2(g) \tag{Eq 5}$$

$$Cu^+(aq) + H_2O_2(aq) \leftrightarrow Cu^{2+}(aq) + O_2(g) + OH^-(aq) + {}^{\bullet}OH(aq) \tag{Eq 6}$$

From reaction (6), the reactive oxide species are the hydroxide ion (OH^-) and the hydroxyl radical ($^{\bullet}OH$). Copper oxide may be restored to the solid form after the following reaction:

$$Cu^{2+}(aq) + O^{2-}(aq) \leftrightarrow CuO(s) \qquad K_{eq} = 1.2 \times 10^{9}. \tag{Eq 7}$$

All the reactions presented are reversible. The equilibrium constants (K_{eq}) indicate the spontaneity of the forward reaction. Higher K_{eq} values indicate that the forward reaction will be more likely to occur. Reaction (2) will be slow in the forward direction since the O_2^- ion is unstable and will dissociate into gaseous oxygen and an electron. The reactive oxide species (OH^-,$^{\bullet}OH$) produced after reaction (6) are extremely oxidative, and will attack most

biological molecules (Ref 10). As they attack molecules present in the PAK cells and are consumed, Le Châtelier's principle predicts that reaction (6) will be driven in the forward direction to adjust to the disturbance in chemical equilibrium. This adjustment will produce additional reactive oxide species for further biological attack. Reaction (7) shows that, based on the large K_{eq} value, the production of CuO is favored, which will restore the oxide in the reaction cycle for further production of reactive oxide species.

As shown in Fig. 6, light-irradiated TiO_2-Cu composite coatings showed greater bactericidal activity than those samples held in a dark chamber. Ohko et al. (Ref 28) have suggested that irradiated TiO_2 may also produce reactive oxygen species as follows:

$$TiO_2(s) + hf \leftrightarrow TiO_2(s) + e^- + h^+, \quad \text{(Eq 8)}$$

where h is Planck's constant (6.63×10^{-34} m^2 kg/s), f is the frequency of the white light radiation, and h^+ are electron holes on the surface of the TiO_2.

Beyond reaction (8), two additional steps will occur:

$$H_2O(l) + h^+ \leftrightarrow {}^{\bullet}OH(aq) + H^+(aq) \quad \text{(Eq 9)}$$

$$O_2(g) + e^- \leftrightarrow O_2{}^-(aq) \quad \text{(Eq 10)}$$

Reaction (9) shows that additional $^{\bullet}OH$ radicals will be produced to accelerate the degradation of PAK cells. Furthermore, the $O_2{}^-$ ions formed in reaction (10) will probably participate in the copper-catalyzed reaction (5) to drive the reaction to produce Cu^+ ions. The cuprous ions (Cu^+) produced from reaction (5) will drive reaction (6) in the forward direction, in accordance with Le Châtelier's principle, to produce more OH^- ions and $^{\bullet}OH$ radicals. The combined effect of the production of OH^- ions and $^{\bullet}OH$ radicals from the copper-catalyzed Haber-Weiss-type reaction mechanism and the light irradiation of TiO_2 will result in increased bactericidal activity of TiO_2-Cu composite coatings exposed to white light as compared to pure, bulk copper (see Fig. 6).

Other possible side reactions may occur after reactions (9) and (10). Given the high reactivity of the $^{\bullet}OH$ radical species, they may combine to give:

$${}^{\bullet}OH(aq) + {}^{\bullet}OH(aq) \leftrightarrow H_2O_2(aq) \quad \text{(Eq 11)}$$

From reaction (10), the following reaction mechanism to form additional dihydrogen peroxide may also occur:

$$O_2{}^-(aq) + {}^{\bullet}OH(aq) \leftrightarrow {}^{\bullet}O_2H(aq) \quad \text{(Eq 12)}$$

$${}^{\bullet}O_2H(aq) + {}^{\bullet}O_2H(aq) \leftrightarrow H_2O_2(aq) + O_2(g) \quad \text{(Eq 13)}$$

The dihydrogen peroxide may participate in reaction (6) to drive the production of additional OH^- ion and $^{\bullet}OH$ radical species.

PAK bacterial cells will probably be more actively attacked by the more reactive $^{\bullet}OH$ radical species. Hydroxyl radicals are extremely reactive, with a half life of $t_{1/2} = 10^{-9}$ s at 37 °C (Ref 29), and they will readily react with almost any biological molecule (Ref 10). It is proposed that cellular integrity will be compromised by first attacking the peptidoglycan layer in the cell wall that protects the bacteria. The general structure and architecture of a typical peptidoglycan molecule has been presented by Vollmer et al. (Ref 30). Since hydroxyl radicals show little discrimination in the organic functional groups that they attack, devising an exact chemical mechanism of cell destruction is difficult. Figure 8 shows a proposed mechanism in which $^{\bullet}OH$ radicals attack the outer peptidoglycan layer of a PAK bacterial cell, resulting in chain polymerization reactions that cause damage to the cell wall. In the mechanism, it is proposed that the radical will attack the hydroxyl group since it is in a primary (1^o) position and attached to a small methyl side group attached to the ring. The possibility exists that another $^{\bullet}OH$ radical will attack the methyl group in the secondary amide (see Fig. 8). These functional groups were chosen because the $^{\bullet}OH$ radical may favor attacking the hydrogen atoms in these groups due to the large dipole moments that will exist around the atoms. The hydrogen atoms in

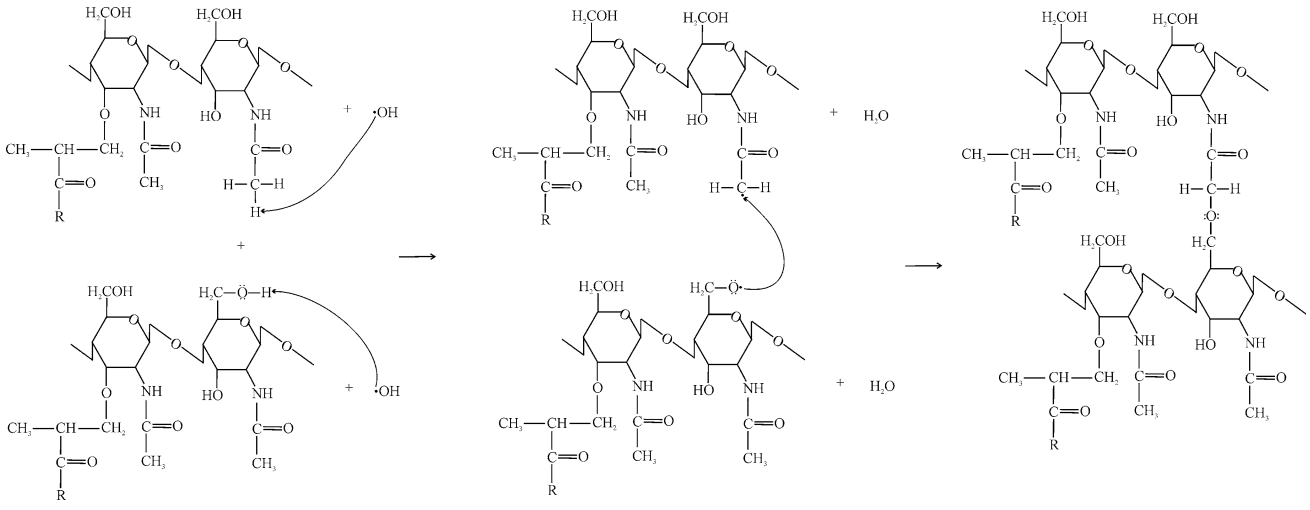

Fig. 8 Proposed reaction mechanism for the attack of the peptidoglycan layer of the PAK cell wall by hydroxyl radicals

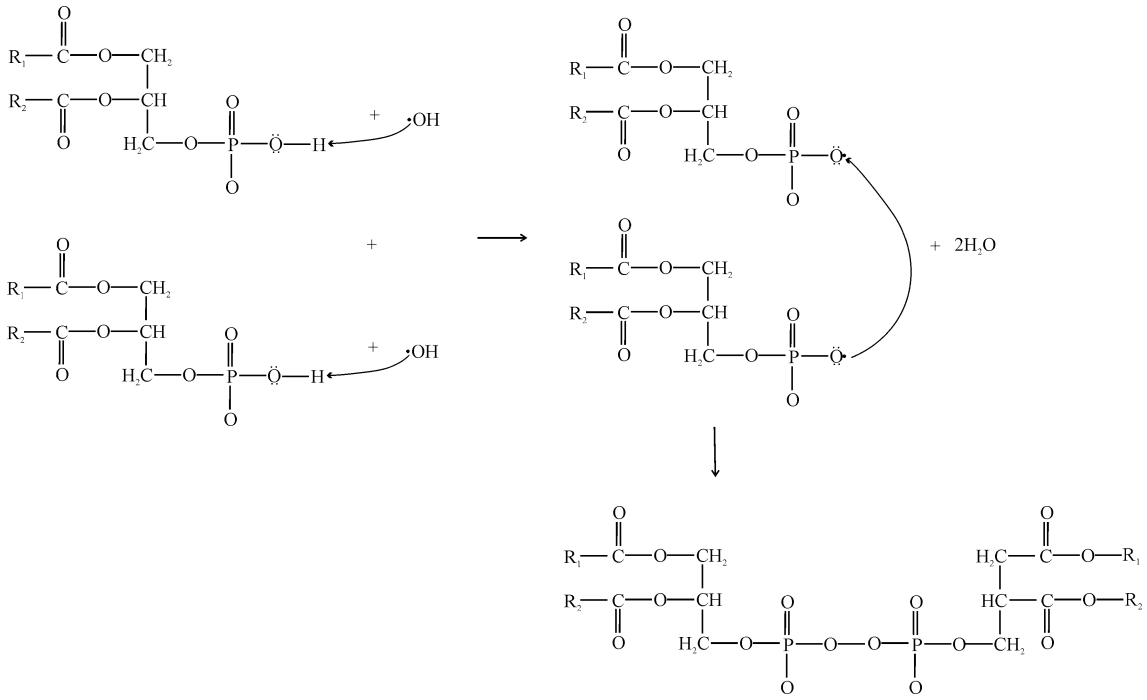

Fig. 9 Proposed reaction mechanism for the attack of phospholipid molecules in the PAK cell membrane by hydroxyl radicals

these functional groups are bonded directly or indirectly to highly electronegative elements such as oxygen or nitrogen, and will possess strong partial positive charge (δ+). This will be sufficient to promote attack by highly reactive and electron-rich •OH radicals. The radicals may also have attacked other functional groups in the peptidoglycan structure.

In Gram negative bacteria such as PAK, there is a peptidoglycan layer sandwiched between an inner cell membrane and an outer cell wall. The membrane consists primarily of phospholipids. Due to the highly reactive nature of the hydroxyl radical, attack of phospholipid molecules will occur. Figure 9 shows a proposed mechanism for the attack of phospholipid molecules by hydroxyl radicals. Similar to Fig. 8, it is proposed that the reactive radicals will have greater affinity to attack the hydrogen on the phosphate group to eventually produce a structure similar to a phosphate ester. The production of this new structure from phospholipids that possessed a hydrophilic –OH group will significantly alter the integrity of the cell membrane, resulting in PAK cell destruction.

5. Conclusions

Flame-sprayed nanostructured and conventional titania (TiO_2) coatings were fabricated and their photocatalytic performance against *Pseudomonas aeruginosa* (PAK) bacteria was studied. The performance of TiO_2 coatings containing 5 wt.% copper was also studied. It was found that the introduction of small amounts of copper into the coating microstructure, coupled with white light irradiation of the surface, significantly increased the bactericidal performance of the coatings. This was attributed to the production of reactive oxide species such as the hydroxide ion and hydroxyl radical, which chemically attacked and damaged the cell wall and membrane, killing the bacterial cells.

While the performance of the metal-ceramic composite coatings was noticeable, it was suggested that the copper-free TiO_2 coatings did not destroy a significant amount of cells. This was attributed to the high flame temperatures in the flame spray torch, which facilitated the conversion of anatase phase present in the TiO_2 powder to rutile phase present in the final coatings. Since the anatase phase is the primary phase that is the source of photocatalytic activity of TiO_2, limited bactericidal effects were observed.

This study was an extension of previous work conducted by other investigators. The results presented suggest that a small amount of metal with anti-microbial properties can be added to nanostructured TiO_2 coatings to improve bactericidal activity. However, further work will be required to increase the percentage of the anatase phase of TiO_2 present in the coatings to increase further the bactericidal capabilities of the coating matrix.

Acknowledgments

The authors gratefully acknowledge the assistance of Miss. Mandy Wan with a preliminary study with rough nanostructured TiO_2 samples. The authors also thank Dr. Roger S. Lima and Dr. Stefan Pukatzki for reviewing the draft manuscript. Funding for this project was

provided by the Natural Sciences and Engineering Research Council of Canada (NSERC), the Government of Alberta Small Equipment Grants Program (SEGP), and the Canada Foundation for Innovation (CFI).

References

1. D. Lindsay and A. von Holy, Bacterial Biofilms Within the Clinical Setting: What Healthcare Professionals Should Know, *J. Hosp. Infec.*, 2006, **64**, p 313-325
2. G.P. Bodey, R. Bolivar, V. Fainstein, and L. Jadeja, Infections Caused by *Pseudomonas aeruginosa*, *Rev. Infec. Dis.*, 1983, **5**, p 279-313
3. E. Vanhaecke, J. Remon, M. Moors, F. Raes, D. de Rudder, and A. van Peteghem, Kinetics of *Pseudomonas aeruginosa* Adhesion to 304 and 316-L Stainless Steel: Role of Cell Surface Hydrophobicity, *Appl. Environ. Microbiol.*, 1990, **56**, p 788-795
4. C. Johansen, P. Falholt, and L. Gram, Enzymatic Removal and Disinfection of Bacterial Biofilms, *Appl. Environ. Microbiol.*, 1997, **63**, p 3724-3728
5. C. Ryder, M. Byrd, and D.J. Wozniak, Role of Polysaccharides in *Pseudomonas aeruginosa* Biofilm Development, *Curr. Opin. Microbiol.*, 2007, **10**, p 644-648
6. Y. Kikuchi, K. Sunada, T. Iyoda, K. Hashimoto, and A. Fujishima, Photocatalytic Bactericidal Effect of TiO_2 Thin Films: Dynamic View of the Active Oxygen Species Responsible for the Effect, *J. Photochem. Photobiol. A*, 1997, **106**, p 51-56
7. P. Evans and D.W. Sheel, Photoactive and Antibacterial TiO_2 Thin Films on Stainless Steel, *Surf. Coat. Technol.*, 2007, **201**, p 9319-9324
8. B. Jeffery, M. Peppler, R.S. Lima, and A. McDonald, Bactericidal Effects of HVOF-sprayed Nanostructured TiO_2 on *Pseudomonas aeruginosa*, *J. Therm. Spray Technol.*, 2010, **19**, p 344-349
9. M.F. Brunella, M.V. Diamanti, M.P. Pedeferri, F. di Fonzo, C.S. Casari, and A. Li Bassi, Photocatalytic Behavior of Different Titanium Dioxide Layers, *Thin Solid Films*, 2007, **515**, p 6309-6313
10. J.A. Imlay, Pathways of Oxidative Damage, *Annu. Rev. Microbiol.*, 2003, **57**, p 395-418
11. L. Brook, P. Evans, H. Foster, M. Pemble, A. Steele, D. Sheel, and H. Yates, Highly Bioactive Silver and Silver/Titania Composite Films Grown by Chemical Vapour Deposition, *J. Photochem. Photobiol. A*, 2007, **187**, p 53-63
12. J.L. Clement and P.S. Jarrett, Antibacterial Silver, *Metal-Based Drugs*, 1994, **5-6**, p 467-482
13. R. Jensen and N. Davidson, Spectrophotometric, Potentiometric, and Density Gradient Ultracentrifugation Studies of the Binding of Silver Ion by DNA, *Biopolymers*, 1966, **4**, p 17-32
14. R.S. Lima and B.R. Marple, Thermal Spray Coatings Engineered from Nanostructured Ceramic Agglomerated Powders for Structural, Thermal Barrier and Biomedical Applications: A Review, *J. Therm. Spray Technol.*, 2007, **16**, p 40-63
15. R.S. Lima, S.E. Kruger, and B.R. Marple, Towards Engineering Isotropic Behaviour of Mechanical Properties in Thermally Sprayed Ceramic Coatings, *Surf. Coat. Technol.*, 2008, **202**, p 3643-3652
16. C.L. Giltner, E.J. van Schaik, G.F. Audette, D. Kao, R.S. Hodges, D.J. Hassett, and R.T. Irvin, The *Psuedomonas aeruginosa* Type IV Pilin Receptor Binding Domain Functions as an Adhesion for Both Biotic and Abiotic Surfaces, *Mol. Microbiol.*, 2000, **59**, p 1083-1096
17. K. Sunada, Y. Kikuchi, K. Hashimoto, and A. Fujishima, Bactericidal and Detoxification Effects of TiO_2 Thin Film Photocatalysts, *Environ. Sci. Technol.*, 1998, **32**, p 726-728
18. N. Berger-Keller, G. Bertrand, C. Filiare, C. Meunier, and C. Coddet, Microstructure of Plasma-Sprayed Titania Coatings Deposited from Spray-Dried Powder, *Surf. Coat. Technol.*, 2007, **168**, p 281-290
19. A. Fujishima and K. Honda, Electrochemical Photolysis of Water at a Semiconductor Electrode, *Nature*, 1972, **238**, p 37-38
20. G. Yang, C. Li, F. Han, and A. Ohmori, Microstructure and Photocatalytic Performance of High Velocity Oxy-Fuel Sprayed TiO_2 Coatings, *Thin Solid Films*, 2004, **466**, p 81-85
21. P. Amézaga-Madrid, G. Nevarez-Moorillon, E. Orrantia-Borunda, and M. Miki-Yoshida, Photoinduced Bactericidal Activity Against *Pseudomonas aeruginosa* by TiO_2 Based Thin Films, *FEMS Microbiol. Lett.*, 2002, **211**, p 183-188
22. S. Kuroda, J. Kawakita, M. Watanabe, and H. Katanoda, Warm Spraying—A Novel Coating Process Based on High-Velocity Impact of Solid Particles, *Sci. Tech. Adv. Mater.*, 2008, **9**, p 033002
23. A.G. Gaynor, R.J. Gonzalez, R.M. Davis, and R. Zallen, Characterization of Nanophase Titania Particles Synthesized Using In Situ Steric Stabilization, *J. Mater. Res.*, 1997, **12**, p 1755-1765
24. A. Ozturk and B. Cetegen, Experiments on Ceramic Formation from Liquid Precursor Spray Axially Injected into an Oxy-Acetylene Flame, *Acta Mater.*, 2005, **53**, p 5203-5211
25. M.J. Domek, M.W. LeChevallier, S.C. Cameron, and G.A. McFeters, Evidence for the Role of Copper in the Injury Process of Coliform Bacteria in Drinking Water, *Appl. Environ. Microbiol.*, 1984, **48**, p 289-293
26. S.I. Liochev and I. Fridovich, The Haber-Weiss Cycle—70 Years Later: An Alternative View, *Redox Rep.*, 2002, **7**, p 55-57, 59-60
27. L. McDowell and H. Johnston, The Solubility of Cupric Oxide in Alkali and the Second Dissociation Constant of Cupric Acid. The Analysis of Very Small Amounts of Copper, *J. Am. Chem. Soc.*, 1936, **58**, p 2009-2014
28. Y. Ohko, K. Hashimoto, and A. Fujishima, Kinetics of Photocatalytic Reactions Under Extremely Low-Intensity UV Illumination on Titanium Dioxide Thin Films, *J. Phys. Chem. A*, 1997, **101**, p 8057-8062
29. A. Boelsterli, *Mechanistic Toxicology: The molecular Basis of How Chemicals Disrupt Biological Targets*, CRC Press, Florida, 2007, p 125-148
30. W. Vollmer, D. Blanot, and M.A. de Pedro, Peptidoglycan Structure and Architecture, *FEMS Microbiol. Rev.*, 2008, **32**, p 149-167